



A model for investigating developmental eye repair in *Xenopus laevis*

Cindy X. Kha, Philip H. Son, Julia Lauper, Kelly Ai-Sun Tseng*

School of Life Sciences and Nevada Institute of Personalized Medicine, University of Nevada, Las Vegas, 4505 South Maryland Parkway, Box 454004, Las Vegas, NV 89154, United States

ARTICLE INFO

Keywords:

Eye
Neural repair
Development
Retina
Xenopus
Developmental regulation
Regeneration

ABSTRACT

Vertebrate eye development is complex and requires early interactions between neuroectoderm and surface ectoderm during embryogenesis. In the African clawed frog, *Xenopus laevis*, individual eye tissues such as the retina and lens can undergo regeneration. However, it has been reported that removal of either the specified eye field at the neurula stage or the eye during tadpole stage does not induce replacement. Here we describe a model for investigating *Xenopus* developmental eye repair. We found that tailbud embryos can readily regrow eyes after surgical removal of over 83% of the specified eye and lens tissues. The regrown eye reached a comparable size to the contralateral control by 5 days and overall animal development was normal. It contained the expected complement of eye cell types (including the pigmented epithelium, retina and lens), and is connected to the brain. Our data also demonstrate that apoptosis, an early mechanism that regulates appendage regeneration, is also required for eye regrowth. Treatment with apoptosis inhibitors (M50054 or NS3694) blocked eye regrowth by inhibiting caspase activation. Together, our findings indicate that frog embryos can undergo successful eye repair after considerable tissue loss and reveals a required role for apoptosis in this process. Furthermore, this *Xenopus* model allows for rapid comparisons of productive eye repair and developmental pathways. It can also facilitate the molecular dissection of signaling mechanisms necessary for initiating repair.

1. Introduction

Regeneration, the ability to replace lost body parts in response to injury, is found in diverse animals. The processes that regulate tissue and organ regeneration are beginning to be understood. However, the reasons for variable capabilities amongst even similar species remain unknown (Agata and Inoue, 2012). An organ that has been studied extensively for its regenerative potential is the eye. The eye is an excellent model especially since its structure is mostly similar between different vertebrate species. Understanding how regeneration occurs in different contexts can provide fundamental insights for stem cell biology, reprogramming, and cell plasticity.

An animal that has high regenerative capabilities is the South African clawed frog, *Xenopus laevis* (Beck, 2012). The *Xenopus* tadpole is a well-established model for studying eye regeneration (Barbosa-Sabanero et al., 2012; Del Rio-Tsonis and Tsonis, 2003; Henry et al., 2008; Tseng, 2017). Its eye has the same structures as found in other vertebrates, including the neural retina, lens, cornea, and pigmented epithelium. Several components of the *Xenopus* eye regenerate after injury. Surgical excision of the tadpole or adult neural retina induced regeneration through activation of retinal progenitor cells and/or transdifferentiation of the retinal pigmented epithelium (Martinez-De

Luna et al., 2011; Vergara and Del Rio-Tsonis, 2009; Yoshii et al., 2007). Similarly, removal of the lens also resulted in regeneration through transdifferentiation of the corneal epithelium cells (Day and Beck, 2011; Freeman, 1963; Hamilton et al., 2016).

Most eye repair studies have focused on understanding the regeneration of mature tissues such as the retina and lens. However, the repair capabilities of *Xenopus* embryos have not been investigated in detail. This may be in part due to the complex coordination of tissue interactions that is required for eye formation. After eye field specification during *Xenopus* neurulation, interactions between two tissues, the neuroectoderm (an outgrowth of the developing brain) and the surface ectoderm are required to form the eye properly (Heavner and Pevny, 2012).

There have been examinations of the regrowth ability of the *Xenopus* eye in embryos and tadpoles. Several studies found that after partial eye removal during late embryonic and tadpole stages, eye size recovered during a span of several weeks prior to adulthood (Berman and Hunt, 1975; Feldman et al., 1975; Underwood and Ide, 1992; Wunsh and Ide, 1990). Other reports indicated that eye growth did not occur after surgical ablation in *Xenopus*, nor *Rana* (leopard frog) embryos (Constantine Paton and Ferrari-Eastman, 1981; Currie and Cowan, 1974; Wetts et al., 1993). More recently, it was found that if an eye

* Corresponding author.

E-mail address: kelly.tseng@unlv.edu (K.A.-S. Tseng).

anlagen is excised from the neurula (developmental stage (st.) 15) embryo, then no eye is made (Vicizian et al., 2009; Zuber, 2010). Interestingly, if the excised eye field tissues were then transplanted into another region of the embryo or cultured *in vitro*, then they developed into an eye (Zuber, 2010). This result showed that the specified eye anlagen can form the correct structure independent of additional signals. The consequences of the removal of a late tailbud embryo eye have also been investigated at st. 33 and st. 40. The embryo developed normally but with a missing eye (Blackiston and Levin, 2013; Sedohara et al., 2003). Together, these recent reports indicated that excision of immature eye tissues results in a failure of the embryo to regrow the lost structures. However, a common view is that regenerative capacity is highest during early life stages and decreases with increasing age. To further assess the eye repair capacity of *Xenopus* during development, we tested st. 27 early tailbud embryos and found that there is successful regrowth of the eye after surgical loss of tissues.

2. Materials and methods

2.1. Embryo culture and surgery

Embryos were obtained via *in vitro* fertilization and were raised in 0.1X Marc's Modified Ringer (MMR, 0.1 M NaCl, 2.0 mM KCl, 1 mM MgSO₄, 2 mM CaCl₂, 5 mM HEPES, pH 7.8) medium (Sive et al., 2000). The eye assay was based on published surgical techniques (Holt, 1980). Embryos at stage (st.) 27 (Nieuwkoop and Faber, 1994) were anaesthetized with MS222 (Sigma). Surgery was performed using fine surgical forceps (Dumont No. 5). An initial cut is first made in the skin surrounding the protruding eye cup and overlying lens placode. The cut is continued around the raised outline of the eye and the protruding tissues are removed. For sham surgery, incisions are made around the perimeter of the raised eye structure but tissues are not excised. After surgery, embryos were transferred into 0.1X MMR, allowed to recover, and then cultured at 22 °C for 1–5 days. The contralateral eye of the embryo served as an internal control. For transplantation assay, a small incision was made at the posterior end along the body axis. The removed eye tissues from the same embryo were grafted to the incision site. Embryos were cultured at 22 °C for 4–5 days.

For chemical treatment, M50054 and NS3694 (Millipore, EMD Biosciences) were used. After experimental surgery at st. 27 and a brief recovery time, embryos were transferred to medium containing the chemical for 24 h. After chemical treatment was completed, embryos were incubated in two changes of medium to remove the inhibitor. Eye regrowth was assayed at 5 days.

2.2. Embryo sectioning, histology and immunofluorescence microscopy

Animals were fixed overnight at 4 °C in MEMFA (100 mM MOPS (pH 7.4), 2 mM EGTA, 1 mM MgSO₄, 3.7% (v/v) formaldehyde) (Sive et al., 2000). For histology or immunostaining, embryos were dehydrated in ethanol, and embedded in Paraplast X-TRA, deparaffinized in xylene, rehydrated in graded ethanol, and stained with hematoxylin and eosin according to (Liu and He, 2013). Paraffin or sucrose embedded tissues were sectioned at 10 µm thickness using a Tissue-Tek Accu-Cut Rotary Microtome. For agarose sectioning, embryos were fixed immediately after surgery in MEMFA and processed as according to (Blackiston et al., 2010). Embryos and tadpoles were embedded in 4–6% agarose and sectioned into 50 µm slices using a Leica vt1000s vibratome.

Wholemout embryos and sections were stained with primary antibodies including: Xen1 (pan-neural antibody, 1:100 dilution, Developmental Studies Hybridoma Bank), anti-Islet-1 (retinal ganglion cells and inner nuclear cell layer, 1:200 dilution, Developmental Studies Hybridoma Bank), anti-Glutamine Synthetase (Müller glia, 1:500 dilution, Sigma-Aldrich), anti-Laminin (basal lamina, 1:300 dilution, Sigma-Aldrich), anti-Calbindin-D-28K (cone photoreceptor, 1:500 dilution, Sigma-Aldrich), anti-Rhodopsin (rod photoreceptor, 1:200

dilution, EMD Millipore), anti-phospho Histone H3 (mitosis marker, 1:500 dilution, EMD Millipore), and anti-activated Caspase-3 antibody (cleaved Caspase-3, 1:300 dilution, Cell Signaling). Alexa fluor conjugated secondary antibodies were used at 1:1000 dilution (Thermo Fisher Scientific). DAPI (4',6-Diamidino-2-Phenylindole, Dihydrochloride, Sigma-Aldrich) and TO-PRO-3 (Molecular Probes) were used for DNA staining.

2.3. Assessment of eye surgery and regrowth

To quantify tissues remaining after surgery, embryos were fixed and the entire head of the animal was sectioned. The embryonic eye was defined as the area immunostained with the neural marker Xen1 and the boundaries highlighted by anti-laminin antibody, indicating the basement membrane surrounding the eye. For each embryo, 2–3 agarose sections of 50 µm thickness were generated. The section containing the largest amount of eye tissues remaining after surgery was measured (in µm) and compared to the area of the contralateral control eye to calculate the percentage of tissue removed in the left eye. To quantify eye regrowth, paraffin sections through the head were stained with hematoxylin and eosin to visualize eye structures. The section containing the largest area of eye tissues was selected from each animal and the eye region on the left (surgery) and right (unoperated control) were measured.

For mitotic counts, all agarose sections were quantified to determine the number of phospho-Histone H3 positive cells in the eye tissues. Images were acquired at the same exposure. The total area for each eye was calculated by measuring the surface area for each eye section and summing the measurements. The total mitotic counts for each eye was then normalized to the total area. The same method was used to assess the number of activated Caspase-3 positive cells in the regrowing control and treatment groups.

To compare the quantity and quality of regrowth in operated eyes versus control eyes, we developed a Regrowth Index (RI) similar to one previously described for tail regeneration (Tseng et al., 2010) (Supplemental Fig. 1). Each regrown eye was scored based on four phenotype categories: full regrowth of an eye (with lens) comparable to an unoperated control eye in structure; partial – minor abnormalities including misshapen and reduction in eye size or incomplete closure of the choroid fissure; weak – no lens and severely reduced and/or malformed eye with most tissues missing; and none – no regenerated tissues visible (See Supplemental Fig. 1). Based on the calculation of the percentage of the number of individuals grouped to each category, each category is then multiplied by 3 (full), 2 (partial), 1 (weak), or 0 (none). The resulting number is a value ranging from 0 to 300, constituting the RI. A value of 0 denotes no regeneration in any of the individuals in the group, while a value of 300 denotes full regeneration in 100% of individuals in a dish.

2.4. Microscopy

Images of whole animals and histological sections were obtained using a Zeiss V20 stereomicroscope with an AxioCam MRc camera. Immunostained tissues were imaged on a Nikon A1R confocal laser scanning microscope (UNLV Confocal and Biological Imaging Core) or a Zeiss Axio Imager 2 microscope. All acquired images were analyzed and/or processed using ZEN Image Analysis software or the open-source FIJI imaging software (Schindelin et al., 2012).

2.5. Statistical analysis

To compare eye regrowth experiments, raw data from scoring was used. Comparison of two treatments was analyzed with Mann-Whitney U test for ordinal data with tied ranks, using normal approximation for large sample sizes. Multiple treatments were compared using a Kruskal-Wallis test, with Dunn's Q corrected for tied ranks. All other

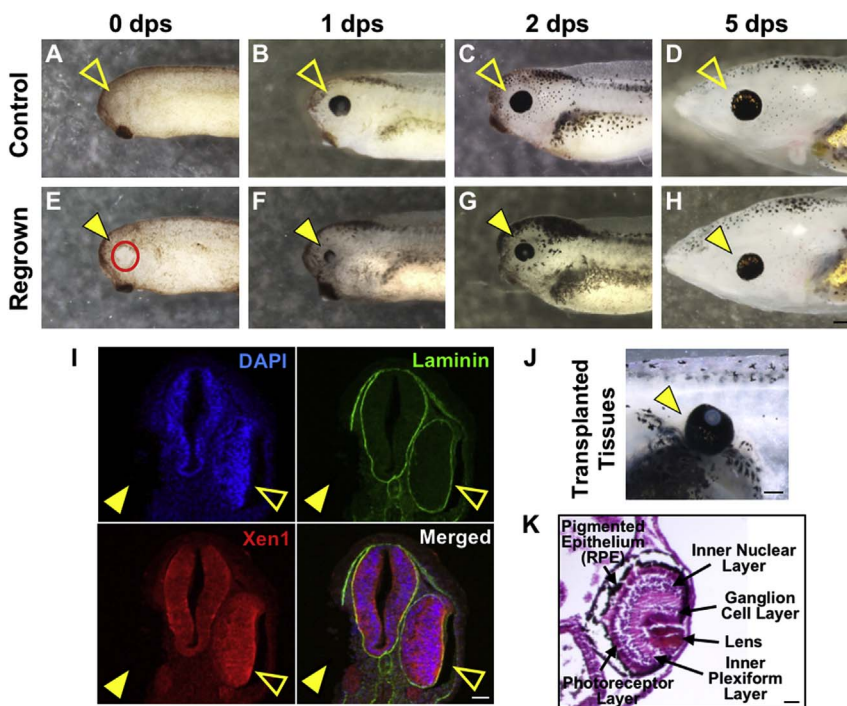


Fig. 1. Tailbud embryos regrow eyes after tissue removal. Images showing normal eye development (A–D) and the eye regrowth process (E–H) starting with st. 27 at the following timepoints: immediately after surgery (0), 1, 2, and 5 days (dps = days post surgery). (A–D) Open arrowheads in the upper panels indicate control, unoperated eyes. (E–H) Closed arrowheads in the bottom panels indicate regrowing eyes. The rate of full eye regrowth (as shown in H and described in [Supplemental Fig. 1](#)) was approximately 93% ($n = 63$). (I) Images are immunostained, transverse sections through the eye plane after surgery. Closed arrowheads indicate surgery site, open arrowheads indicate unoperated eye. Blue color indicates nuclear staining (DAPI). Green color indicates the basal lamina (anti-Laminin), which outlines the optic vesicle. Red color indicates neural tissues (Xen1). (J) Eye tissues removed from a st. 27 embryo were transplanted to its flank at an incision site $\sim 1/2$ from posterior end. By 5 dps, transplanted tissues have a retina and lens similar to the contralateral control eye (not shown) in the same embryo ($n > 20$). (K) Hematoxylin and eosin stained section of transplanted tissues at 5 dps. (A–H) Up = dorsal, down = ventral, left = anterior, right = posterior. (I) Up = dorsal, down = ventral. Scale bars: A–H = 200 μm , I = 25 μm , J = 200 μm , and K = 50 μm .

experiments were analyzed using a Student's t-test.

3. Results

3.1. Tailbud embryo is capable of eye regrowth

To determine whether *Xenopus* embryos can undergo eye repair, eye tissues of the tailbud embryo at developmental stage (st.) 27 were surgically removed using fine forceps to cut around the raised eye structure followed by tissue excision. At 24 h timepoints, the repair response was assessed morphologically ([Fig. 1](#)). After surgery, an open wound was seen where the eye tissues were removed ([Fig. 1E](#)). The wound began to contract within 30 min and was mostly closed by 3 h. After 1 day, the embryo reached approximately st. 33/34 ([Fig. 1B and F](#)). At this timepoint, the normal and uninjured developing eye of the st. 33/34 embryo was larger and outlined by the black retinal pigmented epithelium (RPE) with a lens vesicle at the center (open arrow, [Fig. 1B](#)). In addition, the choroid fissure had begun to close. At the injury site of the 1 day post surgery (dps) embryo, a small eye structure surrounded by RPE was present with a gap in the choroid fissure ([Fig. 1F](#)). By 2 days, the embryo was now at st. 39/40 and its eye had increased in size. For the regrowing eye, the 2 dps structure was more similar in size and morphology to st. 33/34 normal eye, indicating that there was a delay in retinal formation. By 5 dps, the new eye grown at the surgery site (referred to as the “regrown eye”) was comparable to the control eye in age-matched siblings (93% regrowth after surgery, $n > 100$; st. 46/47, swimming tadpole stage) ([Fig. 1H](#)). Together, our data indicated that the tailbud embryo can undergo successful repair to regrow an age-appropriate eye after mechanical injury. Notably, the overall developmental rate and head structures of the injured embryos were similar to the unoperated sibling animals. Thus, the injury did not delay normal development.

3.2. Assessment of eye surgery and regrowth

To quantify the extent of tissue removal after surgery, antibody markers recognizing neural tissues (Xen1, a pan-neural antibody) and the basement membrane (an anti-laminin antibody) were used to visualize the head structure of transverse sections through the injury site

([Fig. 1I](#)). The Xen1 antibody marks neural tissues in st. 34 embryos ([Ruiz i Altaba, 1992](#)). Our data showed that it also identified the developing neural tissues in the st. 27 embryos including the brain and eye cup ([Fig. 1I](#), red signal). An antibody to laminin clearly demarcated the basement membrane that surrounds the eye cup ([Fig. 1I](#), green signal) ([Lunardi et al., 2006](#)). Digital imaging and quantification showed that on average 83% of the eye tissues (eye cup and lens placode) were removed by the surgery on the left eye (yellow arrowhead) of the embryo as compared to the contralateral uninjured control right eye (open arrowhead, $n = 37$, $p < 0.01$). Of the surgeries examined, 17 cases showed an absence of Xen1 or anti-laminin signal at the expected location of the eye ([Fig. 1I](#), yellow arrow compared to uninjured control – open arrow). Together, our data indicated that most of the eye tissues can be removed while still enabling regrowth.

It has been shown that transplantation of the *Xenopus* st. 15 or st. 22 eye primordium to the posterior region of the embryo leads to formation of an eye at the ectopic site ([Blackiston and Levin, 2013; Zuber, 2010](#)). We assessed whether or not the eye tissues excised during surgery are sufficient to form eye structures by transplanting them to the flank of the same embryo. Indeed, the morphology of the ectopic eyes grossly indicated that they have a lens and retinal pigmented epithelium (RPE) ([Fig. 1J](#), $n > 20$). To further examine the internal structure of the ectopic eye, we performed histological analyses. Hematoxylin and eosin staining of sections through an ectopic eye showed that they are capable of forming an eye structure that contained a lens, RPE, and retinal layers ([Fig. 1K](#), $n > 20$). Although this data did not show that the ectopic eye is the same as a normal eye, it demonstrated that sufficient tissues were excised to enable eye development outside of the head region.

3.3. Formation of the regrown eye

A first step towards understanding embryonic eye regrowth is to define the ordered steps in this process. During *Xenopus* eye development, the start of retinogenesis at st. 24 coincides with a decrease in proliferation of the retinal progenitor cells ([Holt, 1980](#)). We hypothesized that differentiation is delayed and proliferation is increased after injury. At st. 27, the embryonic eye contains an eye cup and a differentiating lens placode ([Nieuwkoop and Faber, 1994](#)). As much of eye

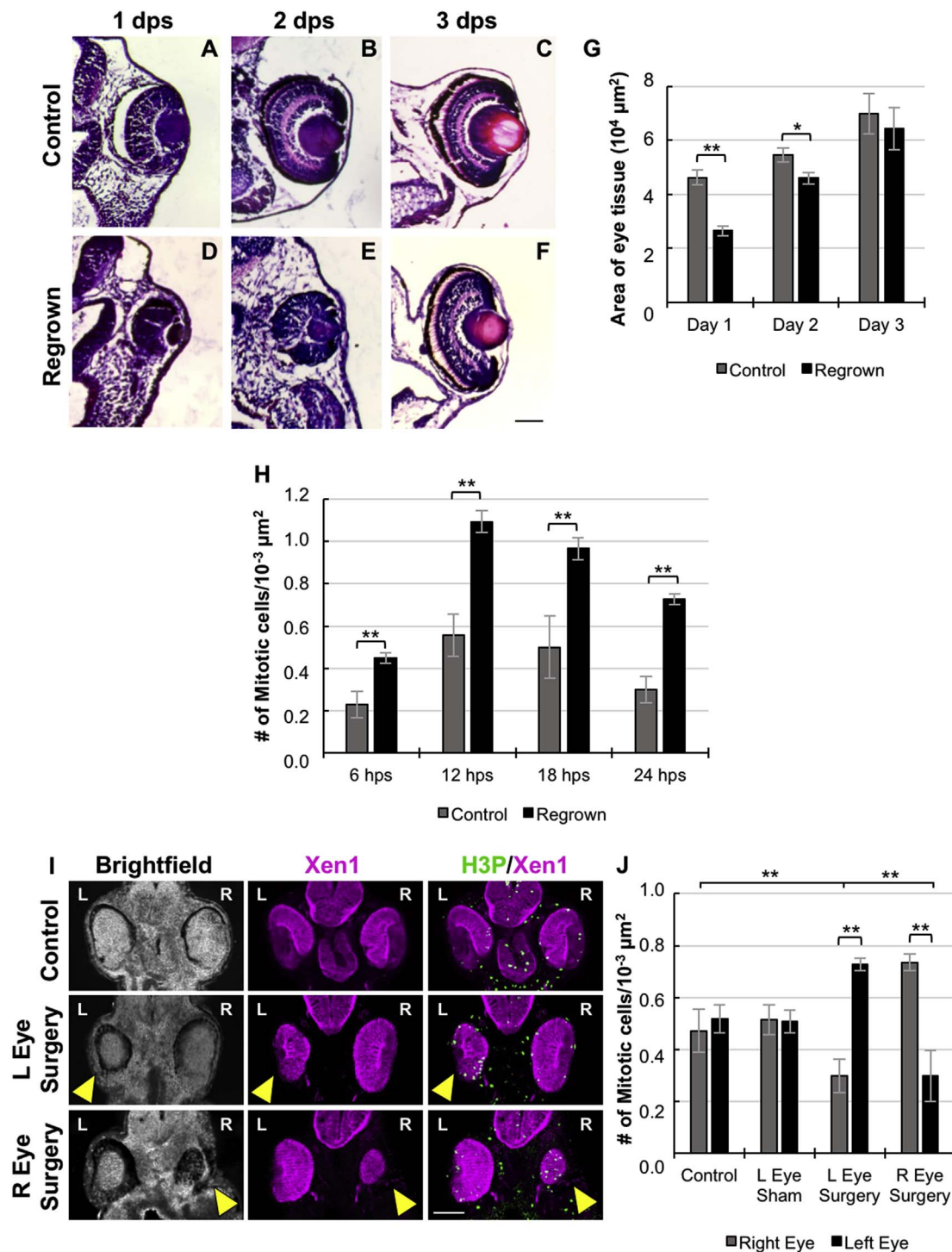


Fig. 2. Proliferation accompanies *Xenopus* eye regrowth. Hematoxylin and eosin stained sections of unoperated eyes (top panels, A–C) compared to age-matched regrowing eyes (bottom panels, D–F). (D) At 1 dps, a small regrowing eye is seen at surgery site. (E) At 2 dps, retinal layer formation is delayed as compared to control (B). (F) By 3 dps, an eye comparable to control is apparent with similar eye organization and size. Representative images are shown. (G) Timecourse of growth rate after surgery as compared to contralateral unoperated eye at day 1 (57.2%, $n = 7$), day 2 (84.4%, $n = 5$), day 3 (92.1%, $n = 6$). * denotes $p < 0.05$, ** denotes $p < 0.01$. Data are means \pm SEM. (H) Quantification of mitoses in the regrowing eye structure at the following timepoints: 6, 12, 18, and 24 hps (hps = hours post surgery). There is an increase in the number of mitotic cells in regions where tissue removal surgery was performed compared to the contralateral control side. ** denotes $p < 0.01$ ($n > 5$ per timepoint). Data are means \pm SEM. (I and J) Assessment of mitoses in the regrowing eye at 24 hps. (I) Mitotic cells are indicated in green by anti-phospho Histone H3 signal. Xen1 indicated neural tissues. Closed arrowheads in the brightfield panels indicated regrowing eyes. (J) Quantification of mitoses in embryos under different conditions as shown. Mitoses are increased in regions where tissue removal surgery was performed, but not in the control or sham-operated eye. L indicates left side. R indicates right side. (A–F, I) Up = dorsal, down = ventral. Scale bars: A–F, I = 50 μm .

development occurs internally, we used histology to examine the cellular changes at the injury site after surgery (Fig. 2A–F). At 1 dps, the embryo had reached st. 33/34, stages when the individual tissue layers of the neural retina began forming (Holt et al., 1988) (Fig. 2A). At this

timepoint, the regrowing eye was significantly smaller (57% of age-matched control, $n = 7$, $p < 0.01$; Fig. 2G) and lacked stratification (Fig. 2D). By 2 dps, the regrowing eye had increased in size and was on average 84% of its age-matched control (Fig. 2G, $n = 5$, $p < 0.05$).

Retinal layer formation appeared to be delayed as the overall structure was more similar to a younger stage (Fig. 2E). By 3 dps, the regrowing eye had largely recovered to an age-appropriate size and its neural retina is comparable in structure to the uninjured control eye ($n = 6$, $p > 0.05$, compare Fig. 2F and C).

The restoration of eye size could result from proliferation at the injury site or nearby cells. To examine proliferation after injury, we assayed cell cycle progression in the regrowing tissues using a known marker of mitosis, anti-phospho-Histone H3 antibody (Saka and Smith, 2001). We counted the number of phospho-Histone H3-positive cells and normalized the counts for area. At each timepoint, mitotic counts for the right and left eyes of control (no surgery) embryos were comparable (Supplemental Fig. S2). In contrast, when the regrowing eye was compared to its contralateral control, there were significant increases in mitotic cell counts during the first 24 hours post surgery (hps) (Fig. 2H). At 6 hps, the regrowing eye showed an increase in mitotic cells (0.45 mitosis per $10^{-3} \mu\text{m}^2$ area) as compared to the contralateral uninjured eye (0.23 mitosis per $10^{-3} \mu\text{m}^2$ area, $n > 5$, $p < 0.01$) (Fig. 2H). At 12, 18, and 24 hps, there were more than double the number of mitoses in the regrowing eye as compared to the contralateral control (Fig. 2H). To confirm that the observed increase in proliferation was due to regrowth and not due to mechanical injury of the eye region, we performed additional controls and assessed mitotic counts at 24 hps (Fig. 2I–J). There was approximately 0.52 mitosis per $10^{-3} \mu\text{m}^2$ area in the unoperated eye cup (Fig. 2I top row, and Fig. 2J), with no significant difference between the left or right eye ($n = 5$ per side, $p = .7$). Sham surgery (making an incision around the eye region without excising the structure) did not alter mitotic counts ($n = 5$ per side, $p = .92$). Eye surgery on the left side of the embryo increased the number of mitotic cells in the regrowing eye (0.73 mitosis per $10^{-3} \mu\text{m}^2$ area) at 24 hps as compared to the contralateral uninjured eye (0.3 mitosis per $10^{-3} \mu\text{m}^2$ area) (Fig. 2I middle row, and Fig. 2J, $n = 5$ per side, $p < 0.01$). There was a similar increase in mitoses in the regrowing eye region when surgery was performed on the right side (Fig. 2I bottom row, and Fig. 2J). Interestingly, there appears to be a decrease in the number of mitoses in the uninjured contralateral eye as compared to normal embryos (Fig. 2J). Together, our data demonstrated that there is a regrowth-specific increase in proliferation in the injured eye. However, this result does not preclude the possibility that there is also increased proliferation in the surrounding area.

3.4. Regrown eyes have the expected structure

To assess whether the regrown eye is structurally similar to a normal eye, we examined the eye structure and cellular composition using histology and tissue markers during the swimming tadpole stage, when the eye is considered to be mature and contained the complement of tissues seen in the adult. Histological sections of regrown eyes at 5 dps showed the same overall morphological structure and tissue layers (including retinal pigmented epithelium, retina, lens, and cornea) as found in control uninjured eyes (Fig. 3A). Using antibody markers that identify retinal cell types, our data showed that the expected retinal cell layers expressed Calbindin and Rhodopsin – markers of cone and rod photoreceptors (Fig. 3B), Islet1 – a marker of retinal ganglion cells (Fig. 3C), and Glutamine Synthetase – a marker of Müller glial cells (Fig. 3D). Together, our results indicate that the regrown eye was highly similar to a normal, mature tadpole eye.

As the regrown eye was morphologically normal, it may be able to transmit visual data. To assess whether the regrown eye is connected to the brain, we examined the optic nerve, the structure that transmits visual information from the retina to the brain (Fig. 4A). We found that the pan-neural antibody, Xen1, identified the optic nerve in tadpoles (Fig. 4B, white arrow). In the regrown eye, the optic nerve innervated into the brain similar to the contralateral control eye, demonstrating that new tissues were likely integrated (Fig. 4A, white arrow indicates optic nerve; left-side yellow arrowhead shows regrown eye, $n > 30$).

Together, our data indicated that the regrowth after surgery restores the eye to a similar age, size, and structure, to the control, unoperated eye by 5 days.

Young swimming *Xenopus* tadpoles show a strong preference for swimming in a white background over a black background (Moriya et al., 1996). Blind tadpoles lose this ability for background preference (Vicizian et al., 2009). This natural visual preference has been used as an assay to test visual response. To grossly assess the potential for visual response of the regrown eyes in swimming tadpoles, we used a behavioral assay as described in (Vicizian and Zuber, 2014). This assay tests whether tadpoles can distinguish between white and black color backgrounds. In our assay, normal uninjured tadpoles spent $> 95\%$ of the time swimming in the white background (Supplemental Fig. S3, $n = 10$). We then examined the swimming preference of tadpoles with one eye. First, we performed surgeries at st. 27 to remove the left eye tissues and then allow regrowth to occur. To test if tadpole visual preference is due to the regrown eye, we then removed the uninjured contralateral (right) eye at st. 40 and did the same for the control siblings. Consistent with previous studies, we observed that eye removal at st. 40 does not induce replacement (Blackiston and Levin, 2013). The removal of the right eye at st. 40 did not affect the regrowth of the left eye. Our data showed that tadpoles with a regrown eye preferred to swim in the white background, similar to control tadpoles with only one unoperated eye (88.2% time spent in white background as compared to 88.4% time spent in white for one-eye controls, $n = 10$ per condition, $p > 0.5$, Supplemental Fig. S3 and Supplemental Video S4). In contrast, blind tadpoles (both eyes removed at st. 40) showed no preference for the white background (Supplemental Fig. S3, $n = 10$, $p < 0.01$ as compared to other groups). Thus the regrown eye showed background color preference. Of note, this behavior could potentially be due to contributions from remnant st. 27 eye cells after surgery.

3.5. Inhibition of apoptosis blocks regrowth

An ongoing focus in regeneration biology is understanding the use of developmental and/or regeneration mechanisms to regrow body structures. It is not known which signals are required for eye regrowth after injury. We sought to determine whether regenerative mechanisms are used for this regrowth process. Apoptosis, programmed cell death, is known to be required for regeneration in a diverse group of animals (Gauron et al., 2013; Li et al., 2010; Pellettieri et al., 2010; Ryoo and Bergmann, 2012; Tseng et al., 2007). It is also a key participant in retinal development and maturation (Gaze and Grant, 1992; O'Driscoll et al., 2006; Walker and Harland, 2009). In contrast, apoptosis does not appear to play a required role in initiating eye formation. Inhibition of developmental apoptosis in *Xenopus* embryos by ectopic expression of the anti-apoptotic gene, Bcl-xL, did not lead to abnormalities (Johnston et al., 2005). We assessed whether apoptosis plays a role in embryonic eye regrowth. First, we examined if apoptosis is present during regrowth. Apoptosis is commonly visualized by using an antibody marker that detects activated Caspase-3, an effector caspase in the cell death cascade (Hayashi et al., 2014; Love et al., 2014; Sirbulescu and Zupanc, 2009; Tseng et al., 2007). To identify apoptotic cells in the regrowing eye tissues, we performed immunostainings with an established anti-activated Caspase-3 antibody that had been successfully used in *Xenopus* (Cervino et al., 2017; Wahl et al., 2015). Four timepoints were examined in the first 24 hps. Consistent with previous studies, a low level of apoptosis was detected in the normally developing eye during st. 27 to st. 33/34 (Fig. 5A) (Hensey and Gautier, 1998). In the regrowing eye, there was a significant increase in apoptotic cells as compared to the uninjured contralateral control at the timepoints assayed (Fig. 5A–B). The highest number of apoptotic cells was seen at 18 hps. This data indicated that apoptosis is upregulated during eye regrowth and supported our hypothesis that it plays a role in this process.

To confirm that apoptosis is functionally required for eye regrowth, we performed chemical loss-of-function experiments. M50054 is a

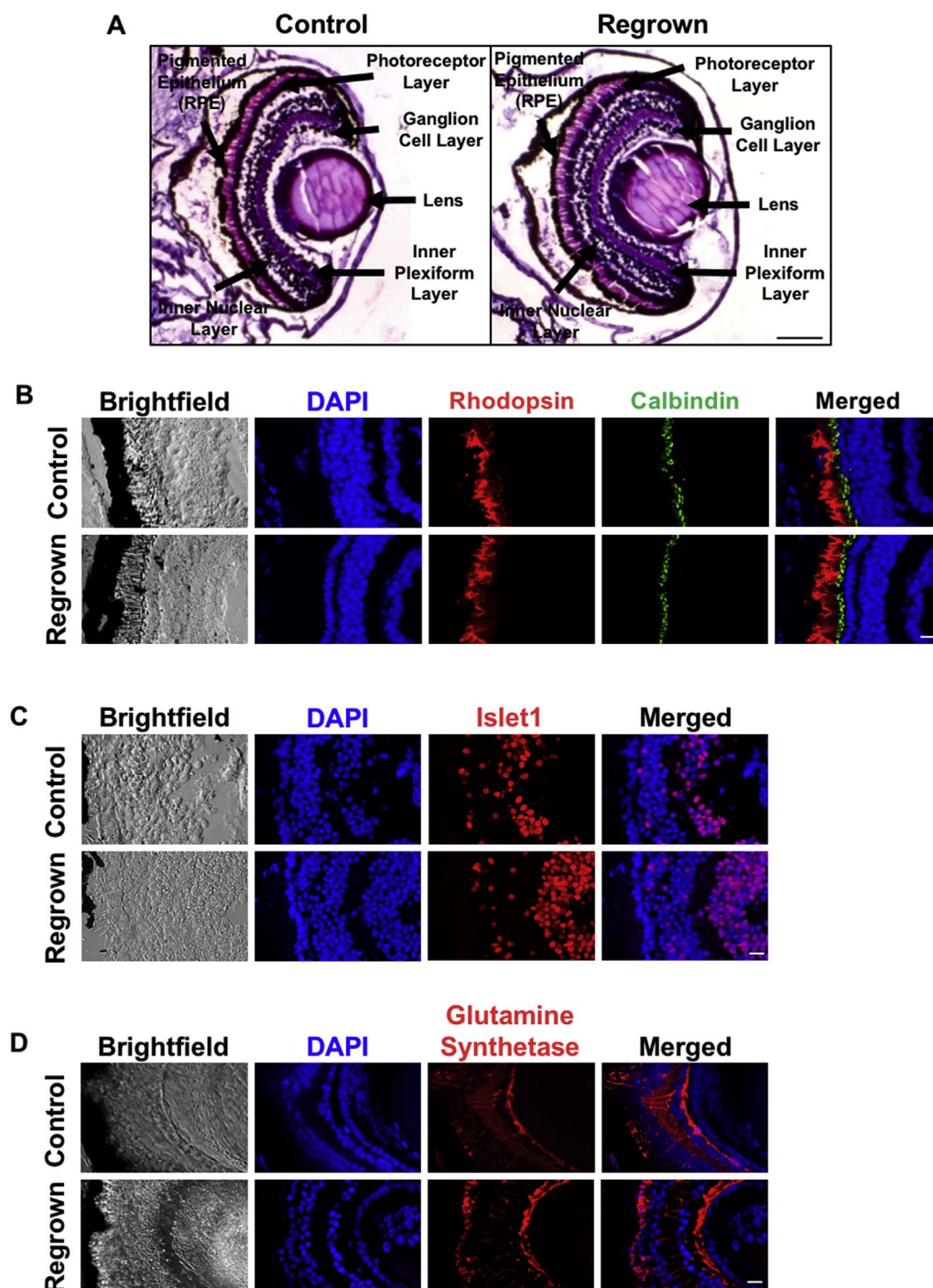


Fig. 3. Regrown eye contains expected cell types. (A) Hematoxylin and eosin stained section of age-matched control (left panel) and regrown eyes at 5 dps (right panel). Regrown eye contains same eye structures compared to unoperated sibling control. (B–D) Identification of retinal cell types in eye regenerates. Dark pigmented tissue surrounding the retina is the retinal pigmented epithelium (RPE). (B) Eye sections stained with DAPI (DNA), anti-Rhodopsin antibody (rod photoreceptors), and anti-Calbindin-D-28K antibody (cone photoreceptors). (C) Eye sections stained with DAPI, anti-Isl1 antibody (identifies retinal ganglion cells, amacrine cells, bipolar cells, and horizontal cells). (D) Eye sections stained with DAPI, and anti-Glutamine Synthetase (Müller glia). (A–D) Up = dorsal, down = ventral. Scale bars: A–D = 50 μ m.

known inhibitor of caspase-3 activation and has been shown to block DNA fragmentation and cell death in a number of cell types; it also rescues chemotherapy-induced alopecia (Tsuda et al., 2001). Exposure of *Xenopus* tadpoles to 35 μ M M50054 inhibited tail regeneration without disrupting overall development (Tseng et al., 2007). Additionally, treatment with M50054 successfully blocked apoptosis and inhibited zebrafish fin and planarian head regeneration (Beane et al., 2013; Gauron et al., 2013). We first titrated the chemical dosage to identify concentrations that enabled normal development and maintained viability of embryos as we did previously for studying tail regeneration (Tseng et al., 2007). The embryos developed normally at dosages of 30 μ M M50054 or less. After eye surgery, st. 27 embryos were treated with M50054 for 24 h and eye regrowth was examined at 5 dps. We found that embryos treated with either 17 or 28 μ M M50054

showed a concentration-dependent inhibition in eye regrowth (Fig. 5C). At 1 dps and 5 dps, the eye tissues in a DMSO-treated regrowing eye was much larger as compared to one exposed to the inhibitor (Fig. 5D). We further assessed the quality of eye regrowth by calculating a Regrowth Index (RI, described in Methods and Supplemental Fig. S1) similar to one that we previously employed for tail regeneration (Tseng et al., 2010). Control regrown eyes showed an RI of 288 ($n = 96$). Treatment with 17 or 28 μ M M50054 resulted in an RI of 198 and 145, respectively (total $n = 191$, $p < 0.01$ as compared to control).

To confirm that regrowth failure was due to apoptotic inhibition and not due to non-specific effects of M50054, we used a second known apoptosis inhibitor with a different mechanism of action. NS3694 is a diacylurea compound that inhibits apoptosis by blocking apoptosome-

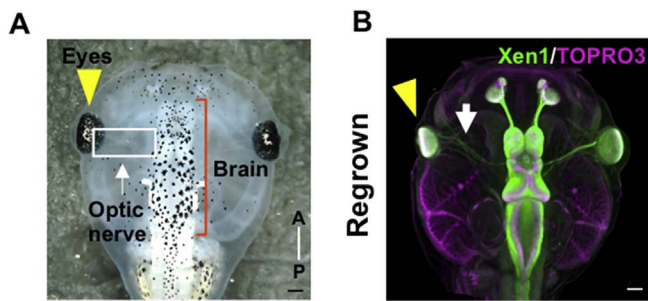


Fig. 4. Regrown eye is connected by an optic nerve. (A) A dorsal view of the tadpole head showing the locations of the eye, optic nerve, and brain. (B) The optic nerve of regrown eye (yellow arrowhead) innervates to the brain, similar to the contralateral, unoperated side. White arrow shows the optic nerve (green) as detected by the Xen1 antibody. Scale bars: A, B = 250 μ m.

mediated caspase activation (Lademann et al., 2003). Exposure to NS3694 successfully inhibited appendage regeneration in both *Xenopus* and zebrafish by reducing apoptosis (Gauron et al., 2013; Tseng et al., 2007). As with M50054, we found that treatment with NS3694 greatly reduced eye regrowth without affecting overall development. At 1 dps and 5 dps, the eye tissues in a DMSO-treated regrowing eye was much larger as compared to one exposed to the inhibitor (Fig. 5D). Compared to control embryos (RI = 283, n = 46), treatment with 40 μ M NS3694 for 24 h after surgery significantly inhibited eye regrowth (Fig. 5E; RI = 165, n = 121, $p < 0.01$), a 60% reduction in the regrowth index. A similar result was seen when embryos were treated with 30 μ M NS3694 (RI = 158, n = 38, $p < 0.01$). In apoptosis, apoptosome formation is the first step required for the activation of the protease pathway used in programmed cell death (Riedl and Salvesen, 2007). It occurs upstream of caspase activation. NS3694 inhibits apoptosome formation and thus would be expected to block caspase-3 activation. Indeed, treatment of embryos with NS3694 consistently reduced the number of activated caspase-3 labeled cells in the eye region by approximately 90% at four different timepoints assayed. (Fig. 5F–G). Together, our data showed that treatment with known apoptosis inhibitors blocked eye regrowth via the inhibition of Caspase-3 activation.

4. Discussion

Our study revealed that *Xenopus* tailbud embryos are capable of successful eye repair after mechanical injury. Previous studies have shown that removal of half of the *Xenopus laevis* eye field during the neurulation stage resulted in a missing eye (Vicgian et al., 2009; Zuber, 2010). This observation suggested that eye field cells are unlikely to undertake repair. One possibility is that the neurula eye field surgery removed or damaged a cellular niche for eye induction whereas the st. 27 surgery is more localized (as the eye area is larger) and maintained the needed structures. Alternatively, the cellular source needed for regrowth does not exist at the neurula stage. The cells of the eye field are known to be multipotent and give rise to all cell types of the retina (reviewed in (Zaghloul et al., 2005)). At st. 27, the heterogeneous retinal progenitor cells represent the majority of the cells in the eye cup even though retinogenesis has begun at st. 24 (Holt et al., 1988; Wong et al., 2009). Given the differing repair capabilities of eye cells at st. 15 and st. 27, there may be molecular changes in the eye progenitor cells after neurulation that enable the tailbud cells to restore eye structures.

The partial excision of the *Xenopus* embryonic or tadpole eye is a classical approach for examining the polarity and establishment of retinotectal connections (Berman and Hunt, 1975; Feldman et al., 1975; Holt, 1980; C. Straznicky et al., 1980). Several studies reported that the partially injured late embryonic/young tadpole eye (st. 32–47) regrew to normal size by adulthood, a span of several weeks (Conway and Hunt, 1987; Feldman et al., 1975; Ide et al., 1983; Underwood et al.,

1992, 1993). It was suggested that this regrowth may be due to proliferation from the ciliary margin zone (CMZ), a peripheral eye region bordering the retina where multipotent stem cells continue to produce retinal cells as part of normal eye growth during development (K. Straznicky and Gaze, 1971). However, this hypothesis has not been examined. In this study, we found that removing the majority of eye tissues in the st. 27 tailbud embryo resulted in rapid regrowth to normal sized eye within 3–5 days (Fig. 1). As the CMZ has not yet formed at st. 27, it is likely that the mechanisms that drive regrowth at st. 27 after surgery differ from regrowth at later stages.

There are key differences between our model and earlier studies that examined partial eye removal. Our surgical technique was modeled after the eye removal surgery performed in (Holt, 1980) where the overlying lens epidermis is removed, which was not the case for earlier studies where partial fragments of the eye were left intact (Berman and Hunt, 1975; Underwood and Ide, 1992). Furthermore, those studies found recovery of eye size occurred before adulthood, over a span of approximately one month. However, the eye regrowth process that we are studying results in size and patterning recovery within only 5 days. This is a significantly faster timeframe and points to a potentially different mechanism for repair than for previous studies. These results suggest that the embryonic *Xenopus* eye is a powerful model for studying developmental eye repair. This model will allow for rapid comparisons of productive repair and developmental pathways in the eye. As *Xenopus* eye development is well-characterized, it will also facilitate the molecular dissection of developmental eye repair mechanisms.

A hallmark of retinal differentiation is that there is an intrinsic developmental clock for histogenesis. In *Xenopus laevis*, chemical inhibition of cell cycle progression during early eye development did not alter the timing of retinogenesis even though the number of eye progenitor cells was greatly reduced (Harris and Hartenstein, 1991). Heterochronic mixing of *Xenopus* embryonic eye cells from different stages *in vivo* and *in vitro* also showed that differentiation timing was not changed and remained unresponsive to external cues (Rapaport et al., 2001). In our study, histological analyses showed that retinogenesis is delayed for at least a day during eye regrowth (compare Fig. 2A–B with Fig. 2D–E). There is also increased mitotic activity at the same time (Fig. 2H). Together, these data suggest that the developmental clock can be altered by injury and/or a proliferative response. Moreover, it is likely that reparative retinogenesis is of shorter duration as retinal layer formation catches up to normal developing eye within 3 days.

Apoptosis is known to be required for regeneration in multiple tissues including *Xenopus* tadpole and newt tails, zebrafish fin, hydra, and mouse skin and liver (Chera et al., 2009; Gauron et al., 2013; Li et al., 2010; Ponomareva et al., 2015; Tseng et al., 2007). The functional role of apoptosis in eye regeneration has not been investigated in detail. Apoptotic cells, identified by DNA fragmentation, were found during the early and late stages of retinal regeneration in adult newts (Kaneko et al., 1999). Our study indicated that apoptosis regulates embryonic eye regrowth in *Xenopus*. We observed a significant increase in apoptosis in the regrowing eye throughout the first 24 h after injury. Treatment with apoptosis inhibitors for the first 24 h after surgery decreased the number of apoptotic cells significantly and was sufficient to block regrowth. However, addition of the inhibitors after 24 h had no effect. This temporal treatment data suggest that apoptosis is required early for the regrowth process, similar to tadpole tail regeneration. A candidate downstream effector driving regrowth could be the Wnt signaling pathway. In hydra, induction of apoptosis after midgastric bisection resulted in the secretion of Wnt3 to drive head regeneration (Chera et al., 2009). In larval zebrafish, active Wnt signaling is required for regenerative proliferation after photoreceptor ablation (Meyers et al., 2012). Further studies are needed to define the role of apoptosis during eye regrowth.

A longstanding question is to understand whether developmental organ regrowth in response to injury (known as regulation) is simply a

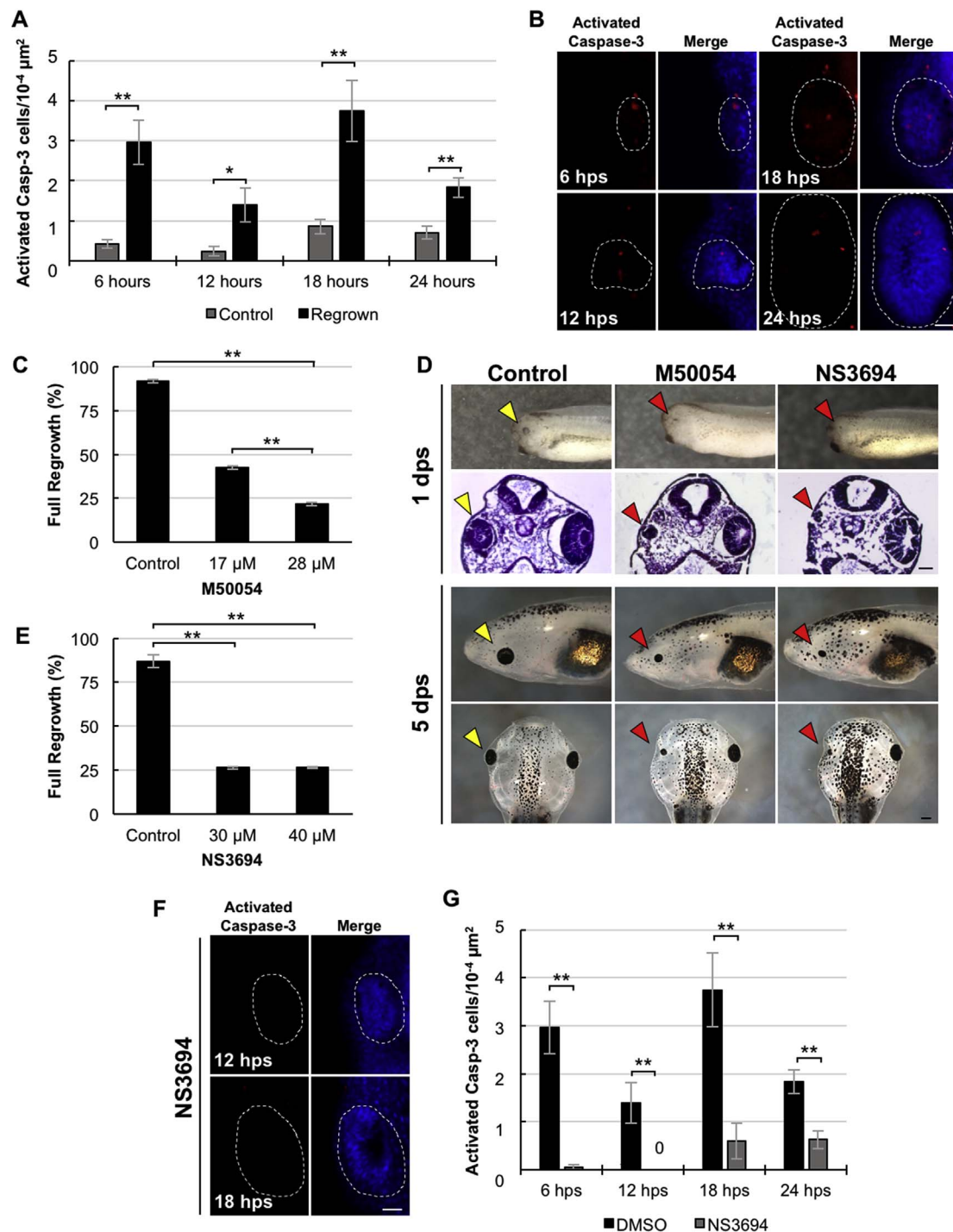


Fig. 5. Apoptosis is required for regrowth. (A) Quantification of apoptotic cells in the regrowing eye structure at the following timepoints: 6, 12, 18, and 24 hps. The activated caspase-3 signal is increased in regions where tissue removal surgery was performed, but not in the contralateral control eye. * denotes $p < 0.05$, ** denotes $p < 0.01$ ($n > 5$ per timepoint). Data are means \pm SEM. (B) Images of activated caspase-3 activity in the regrowing eye. Activated caspase-3 signal is shown in red by anti-cleaved Caspase-3 antibody. DAPI (DNA) is shown in blue. White dashed lines delineate the regrowing eye. (C and E) Effects of treatment of apoptosis inhibitors, M50054 and NS3694, in eye regrowth. ** denotes $p < 0.01$, ($n > 38$ per condition). Data are means \pm SEM. (D) Inhibitor treatment impairs eye regrowth at 1 dps as compared to DMSO-vehicle control regrowing eye. Yellow arrowhead shows control surgery site. Red arrowhead indicates surgery site with inhibitor treatment. Hematoxylin and eosin stained section at region of surgery show differences in regrowing eye tissue with or without treatment. At 5 dps, M50054 and NS3694 severely blocks eye regrowth. (F) Assessment of activated caspase-3 signal in NS3694 treated group show little to no activity. (G) Decrease in number of activated caspase-3 signal in the regrowing eye structure after NS3694 treatment compared to DMSO-vehicle control treatment seen across different timepoints. A zero denotes no signal was detected. ** denotes $p < 0.01$ ($n > 5$ per timepoint). Data are means \pm SEM. Scale bars: B, F = 50 μm , D = 250 μm (brightfield) and 50 μm (H&E).

variation of development. Studies have demonstrated that organ regeneration utilizes a number of developmental mechanisms to restore damaged structures (King and Newmark, 2012; Tanaka and Ferretti, 2009; Tseng and Levin, 2008). However, there are some differences between the two processes. First, developmental repair occurs only as a

response to an unexpected injury that results in loss of body structure (s). Second, initiation of repair may require specific signals not used for normal developmental events. In this study, we found that apoptosis is needed for successful eye regrowth (Fig. 5). Third, repair can occur at a different life stage than the specific developmental events. Thus, the

- 129–141.
- Riedl, S.J., Salvesen, G.S., 2007. The apoptosome: signalling platform of cell death. *Nat. Rev. Mol. Cell Biol.* 8, 405–413. <http://dx.doi.org/10.1038/nrm2153>.
- Ruiz i Altaba, A., 1992. Planar and vertical signals in the induction and patterning of the *Xenopus* nervous system. *Development* 116, 67–80.
- Ryoo, H.D., Bergmann, A., 2012. The role of apoptosis-induced proliferation for regeneration and cancer. *Cold Spring Harbor Perspect. Biol.* 4, a008797. <http://dx.doi.org/10.1101/cshperspect.a008797>.
- Saka, Y., Smith, J.C., 2001. Spatial and temporal patterns of cell division during early *Xenopus* embryogenesis. *Dev. Biol.* 229, 307–318. <http://dx.doi.org/10.1006/dbio.2000.0101>.
- Schindelin, J., Arganda-Carreras, I., Frise, E., Kaynig, V., Longair, M., Pietzsch, T., Preibisch, S., Rueden, C., Saalfeld, S., Schmid, B., Tinevez, J.-Y., White, D.J., Hartenstein, V., Eliceiri, K., Tomancak, P., Cardona, A., 2012. Fiji: an open-source platform for biological-image analysis. *Br. J. Pharmacol.* 9, 676–682. <http://dx.doi.org/10.1038/nmeth.2019>.
- Sedohara, A., Komazaki, S., Asashima, M., 2003. In vitro induction and transplantation of eye during early *Xenopus* development. *Development. Growth & Differentiation* 45, 463–471. <http://dx.doi.org/10.1111/j.1440-169X.2003.00713.x>.
- Sive, H.L., Grainger, R.M., Harland, R.M., 2000. Early Development of *Xenopus laevis*: a Laboratory Manual. Cold Spring Harbor Laboratory Press. Cold Spring Harbor, New York.
- Sirbulescu, R.F., Zupanc, G.K.H., 2009. Dynamics of caspase-3-mediated apoptosis during spinal cord regeneration in the teleost fish, *Apteronotus leptorhynchus*. *Brain Res.* 1304, 14–25. <http://dx.doi.org/10.1016/j.brainres.2009.09.071>.
- Straznicki, C., Gaze, R.M., Keating, M.J., 1980. The retinotectal projections from surgically rounded-up half-eyes in *Xenopus*. *J. Embryol. Exp. Morphol.* 58, 79–91.
- Straznicki, K., Gaze, R.M., 1971. The growth of the retina in *Xenopus laevis*: an autoradiographic study. *J. Embryol. Exp. Morphol.* 26, 67–79.
- Tanaka, E.M., Ferretti, P., 2009. Considering the Evolution of Regeneration in the Central Nervous System, vol. 10. pp. 713–723. <http://dx.doi.org/10.1038/nrn2707>.
- Tsang, A.-S., 2017. Seeing the future: using *Xenopus* to understand eye regeneration. *Genesis* 55, e23003. <http://dx.doi.org/10.1002/dvg.23003>.
- Tsang, A.-S., Adams, D.S., Qiu, D., Koustubhan, P., Levin, M., 2007. Apoptosis is required during early stages of tail regeneration in *Xenopus laevis*. *Dev. Biol.* 301, 62–69. <http://dx.doi.org/10.1016/j.ydbio.2006.10.048>.
- Tsang, A.-S., Beane, W.S., Lemire, J.M., Masi, A., Levin, M., 2010. Induction of vertebrate regeneration by a transient sodium current. *J. Neurosci.* 30, 13192–13200. <http://dx.doi.org/10.1523/JNEUROSCI.3315-10.2010>.
- Tsang, A.-S., Levin, M., 2008. Tail regeneration in *Xenopus laevis* as a model for understanding tissue repair. *J. Dent. Res.* 87, 806–816. <http://dx.doi.org/10.1177/154405910808700909>.
- Tsuda, T., Ohmori, Y., Muramatsu, H., Hosaka, Y., Takiguchi, K., Saitoh, F., Kato, K., Nakayama, K., Nakamura, N., Nagata, S., Mochizuki, H., 2001. Inhibitory effect of M50054, a novel inhibitor of apoptosis, on anti-Fas-antibody-induced hepatitis and chemotherapy-induced alopecia. *Eur. J. Pharmacol.* 433, 37–45.
- Underwood, L.W., Carruth, M.R., Vandecar Ide, A., Ide, C.F., 1993. Relationship between local cell division and cell displacement during regeneration of embryonic *Xenopus* eye fragments. *J. Exp. Zool.* 265, 165–177. <http://dx.doi.org/10.1002/jez.1402650208>.
- Underwood, L.W., Ide, C.F., 1992. An autoradiographic time study during regeneration in fully differentiated *Xenopus* eyes. *J. Exp. Zool.* 262, 193–201. <http://dx.doi.org/10.1002/jez.1402620209>.
- Underwood, L.W., Nelson, P., Noelke, E., Ide, C.F., 1992. Embryonic retinal ablation and post-metamorphic optic nerve crush: effects upon the pattern of regenerated retinotectal connections. *J. Exp. Zool.* 261, 18–26. <http://dx.doi.org/10.1002/jez.1402610104>.
- Vergara, M.N., Del Rio-Tsonis, K., 2009. Retinal regeneration in the *Xenopus laevis* tadpole: a new model system. *Mol. Vis.* 15, 1000–1013.
- Viczian, A.S., Solessio, E.C., Lyou, Y., Zuber, M.E., 2009. Generation of functional eyes from pluripotent cells. *PLoS Biol.* 7, e1000174. <http://dx.doi.org/10.1371/journal.pbio.1000174>.
- Viczian, A.S., Zuber, M.E., 2014. A Simple Behavioral Assay for Testing Visual Function in *Xenopus laevis*. *JoVE*, pp. 1–7. <http://dx.doi.org/10.3791/51726>.
- Wahl, S.E., Kennedy, A.E., Wyatt, B.H., Moore, A.D., Pridgen, D.E., Cherry, A.M., Mavila, C.B., Dickinson, A.J.G., 2015. The role of folate metabolism in orofacial development and clefting. *Dev. Biol.* 405, 108–122. <http://dx.doi.org/10.1016/j.ydbio.2015.07.001>.
- Walker, J.C., Harland, R.M., 2009. microRNA-24a is required to repress apoptosis in the developing neural retina. *Genes Dev.* 23, 1046–1051. <http://dx.doi.org/10.1101/gad.1777709>.
- Wetts, R., Kook, J.H., Fraser, S.E., 1993. Proportion of proliferative cells in the tadpole retina is increased after embryonic lesion. *Dev. Dyn.* 198, 54–64. <http://dx.doi.org/10.1002/aja.1001980106>.
- Wong, L.L., Rapaport, D.H., Wong, L.L., Rapaport, D.H., 2009. Defining retinal progenitor cell competence in *Xenopus laevis* by clonal analysis. *Development* 136, 1707–1715. <http://dx.doi.org/10.1242/dev.027607>.
- Wunsh, L.M., Ide, C.F., 1990. Fully differentiated *Xenopus* eye fragments regenerate to form pattern-duplicated visuo-tectal projections. *J. Exp. Zool.* 254, 192–201. <http://dx.doi.org/10.1002/jez.1402540211>.
- Yoshii, C., Ueda, Y., Okamoto, M., Araki, M., 2007. Neural retinal regeneration in the anuran amphibian *Xenopus laevis* post-metamorphosis: transdifferentiation of retinal pigmented epithelium regenerates the neural retina. *Dev. Biol.* 303, 45–56. <http://dx.doi.org/10.1016/j.ydbio.2006.11.024>.
- Zaghloul, N.A., Yan, B., Moody, S.A., 2005. Step-wise specification of retinal stem cells during normal embryogenesis. *Biol. Cell* 97, 321–337. <http://dx.doi.org/10.1042/BC20040521>.
- Zuber, M.E., 2010. Eye field specification in *Xenopus laevis*. *Curr. Top. Dev. Biol.* 93, 29–60. <http://dx.doi.org/10.1016/B978-0-12-385044-7.00002-3>.